International Journal of ChemTech Research
CODEN (USA): IJCRGG ISSN: 0974-4290
Vol.8, No.1, pp 249-260, 2015

Synthesis, Crystal Structure and Antimicrobial Activities of an Ionic Salt N-(2-Pyridyl)Piperazinium Tetrachlorocuprate(II) Containing Dimeric Anion and DFT Calculations

N. Dhanam[1]* and A. Thamaraichelvan[2]

[1]D.K.M. College for women (Autonomous), Vellore-632001, Tamilnadu, India
[2]Thiagarajar College, Madurai-625009, Tamilnadu India

Abstract: A new ionic salt of N-(2-pyridyl)piperazinium tetrachlorocuprate(II) (PPCC) has been synthesized and characterized by UV-Visible, FT-IR, TGA and NMR analyses. The structure was confirmed by single crystal XRD. It is monoclinic, with the space group of $P2_1/c$ with the values of a = 9.194(5) Å; b = 16.152(5) Å; c = 9.471(5) Å and α = 90°, β = 99.254(5) °, 90° = 90.000(5) ° and Z = 4. The anion shows a chloride-bridged binuclear structure with Cu….Cu distance of 3.935 Å; the two Cu(II) ions have distorted trigonal bipyramidal geometry. Extensive hydrogen bonding between the cation and the tetrachlorocuprate(II) unit found to stabilize the structure. DFT calculations and the anti microbial activities of the titled compound were also carried out.
Keywords: Single crystal XRD, DFT calculations, piperazine derivatives, anti microbial activities and hydrogen bonding.

Introduction

Piperazine and its derivatives have extensively been investigated in view of their biological activities[1]. Further, they have a wide range of applications in the treatment of functional diseases and exhibit anthelmintic, antibacterial and insecticidal activities[2]. Studies on chlorocuprates of organic cations have focused attention on their significant role in catalysis[3], phase transitions[4], non-linear optics[5], thermochromism[6], antiferromagnetism[7] and modeling of Cu(II) metalloproteins[8]. Moreover, a number of chlorocuprate(II) compounds involving heterocyclic amines as ligands have been reported[9].

The tetrachlorocuprate(II) chromophore exhibits a variety of interesting stereochemical features like pseudotetrahedral[10], square planar[11], trigonal bipyramidal[12] and tetragonally elongated octahedral, in which $CuCl_6$ units linked to form two dimensional layer structure[13]. The geometry of the $[CuCl_4]^{2-}$ anion can be determined by many factors like the size of cation, Jahn-Teller effect, electrostatic repulsion between Cl atoms, crystal packing forces and hydrogen bonding[14]. According to the literature for bulky organic cations, the anions exist as dimers or discrete monomers with strictly four-coordinated copper atom[15]. While Jahn-Teller effect lowers the symmetry of $[CuCl_4]^{2-}$ anion below tetragonal[16], whereas square planar geometry appears to be strongly stabilized by hydrogen bonding with the organic cations and crystal packing forces[17]. The structural variations observed in tetrachlorocuprates(II) are mainly influenced by the size and hydrogen bonding nature of medium sized organic cations.

Herein we report the synthesis and characterization of binuclear chlorocuprate with N-(2-pyridyl)piperazine ligand. The geometry of Cu^{2+} lies between square pyramidal and distorted trigonal bipyramidal geometry. Similar type of structure has been found for chlorocuprate(II) of guanidinium salt[18].

Experimental

Materials and methods

The chemicals and solvents were obtained commercially from Merck and Sigma Aldrich and were used as such without any further purification. The CHNS analyzer, Varian Micro cube and LECO CHNS-932 instrument was used to determine the percentage of C, H and N. The electronic spectrum was recorded using a JASCO 530V UV-Visible spectrophotometer in the range of 200-1000 nm employing a quartz cell of 1 cm path length. Acetonitrile was used as a reference. The FT-IR spectral measurement was performed in a JASCO FT-IR 460 plus spectrophotometer employing KBr pellets in the range of 4000-400 cm^{-1}. Thermo gravimetric and Differential Thermal analysis were carried out using NETZSCH STA 409/C/CD instrument in the range of 30-600˚C with platinum crucible in the presence of air and a scanning rate of 10.0˚C min^{-1}. The molar conductivity was measured in DCM 900 using freshly prepared complex solution in DMF. The NMR spectrum was recorded on Bruker DPX 400 (^{1}H 400 MHz) spectrometer using DMSO as solvent.

Single crystal X-ray data were collected on a Nonius MACH3 diffractometer with ω-2θ scans. All measurements were made with graphite monochromated Mo-Kα radiation. Cell parameters and an orientation matrix for data collection were obtained from a least squares refining on F^2 using SHELXL-97[19]. The structure solution was performed by fourier Techniques. While the non-hydrogen atoms were refined anisotropically, hydrogen atom positions were calculated using a riding model refined isotropically. The crystal structure was solved using SHELXS and SHELXL programs[19].

DFT calculations were performed with a hybrid functional B3LYP (Becke's three parameters hybrid functional using the LYP correlation functional) at basis set 6-311+G** by the Bernay method[20], were performed with the Gaussian 03 software package[21].

The antibacterial activity for the titled compound was tested against *Escherichia coli, Staphylococcus aureus* and *Pseudomonas aeruginosa* following the standard disc diffusion method[22]. Active cultures were prepared by transferring a loopful of culture to test tubes containing Muller Hinton Broth (MHB) that was incubated without agitation for 24 h at 37 °C. Muller Hinton Agar (MHA) plates were prepared and the inoculum (18-24 h old broth culture) of the bacteria was spread on them using sterile swab. The extract (20 µl) loaded 6 mm disc was placed on the plates using sterile forceps. The discs were loaded with the respective solvent and Gentamycin served as controls and they were also placed on the same plate. The plates were then incubated at 37 °C for 24 h and the inhibition zone was measured in mm.

The antifungal activity was studied against two fungal cultures of *Colletotrichum* and *Fusarium* species. Sabouraud dextrose agar was prepared, sterilized and the culture plates were prepared in a similar way as that used for Muller Hilton Agar. After solidification of the media, respective fungal spore suspensions were transferred to petri plates. The wells were made in the media with the help of a sterile metallic borer with at least 24 mm in diameter. Concentration of 50 μL of the test sample (10 mg/mL) in DMSO was introduced in the wells. The plates were incubated at 30°C for 72 hours. The results were recorded as zones of inhibition in mm[23]. The experiments were repeated for 100 μL concentration.

Synthesis N-(2-pyridyl)piperazinium tetrachlorocuprate(II) complex

An 10 mL aqueous solution of $CuCl_2.2H_2O$ (1.7 g, 10 mmol) was mixed slowly with N-(2-pyridyl)piperazine (2.063 g, 10 mmol) in deionized water which yields a dark brown colored precipitate. It was then dissolved in 1 mL of (10 N) concentrated hydrochloric acid followed by the addition of in 10 mL of deionized water in drops via a Pasteur pipette to the mixture. The resulting clear solution was filtered and kept at room temperature. Brown crystals of N-(2-pyridyl)piperazinium tetrachlorocuprate(II) were obtained. The crystals were washed with 95% ethanol, diethyl ether and dried. Yield: 90%. Anal.Calc. for C_{18} H_{30} N_6 Cu_2 Cl_8 (F.wt.370.58) : C 29.12, H 4.10, N 11.12, Found: C 29.14, H 4.045, N 11.33. μ_{eff} = 1.73.

Results and Discussion

The compounds is brown colored crystals and stable at ambient temperature and are insoluble in common organic solvents but are soluble in coordinating solvents such as DMSO and DMF. The conductivity measurement of the titled compound was made in water showed molar conductivity value of 143 Ω^{-1} cm^2 mol^{-1} representing that the compound has the property of good electrolytic in nature[24,25].

UV-Visible spectrum

The electronic spectrum of PPCC is given in Figure 1. The peak at 463 nm is assigned to the d-d transition of the Cu(II) ion. The bands observed at 221 nm and 245 nm are due to π-π^* transitions of the pyridine ring present in the ligand. The 303 nm peak may correspond to $Cu^{(II)} \rightarrow Cl^-$ ligand field charge transfer transition as presented in literature for other chlorocuprate(II) [26].

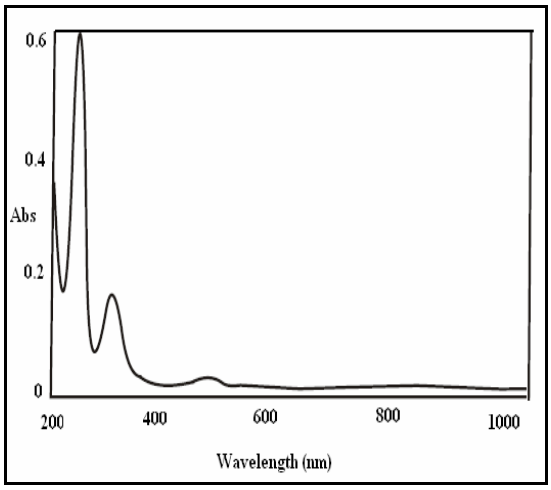

Figure. 1: Electronic spectrum of PPCC

FTIR spectrum

The FTIR spectrum of PPCC (Figure 2) exhibits the symmetric and asymmetric stretching modes of NH_2 group at 3455 and 3266 cm^{-1} in free ligand are found to be downshifted to 3420 and 3233 cm^{-1} respectively in PPCC due to H-bonding by N-H moiety with Cl atoms. The C-H stretching vibrations are observed in the range of 3020-3100 cm^{-1}. The bands observed at 1136 and 1330 cm^{-1} are due to C-H bending vibrations. The $\nu_{C=C}$ bands are observed at 1594 cm^{-1} and the torsional vibration at 440 cm^{-1}. The band at 995 cm^{-1} is ascribed to the C-H wagging mode. Appearance of a peak at 788 cm^{-1} associated with the C-Cl bonds. The 1570 cm^{-1} peak may be due to deformation mode of NH_2. All modes show considerable shifts in comparison to unprotonated N-(2-pyridyl)piperazine (3266, 3174, 3027, 2655, 1841, 1675, 1594, 1444, 1301, 1154, 1114, 995, 941, 755, 742 and 680 cm^{-1}). The differences could be attributed to the protonation of N atoms. This observation along with the broadening of the peaks indicate the presence of a strong hydrogen bonding interaction between the N^+--H and Cu-Cl units as revealed by the crystal structures. Similar observations have been made by Willett et *al*.[22].

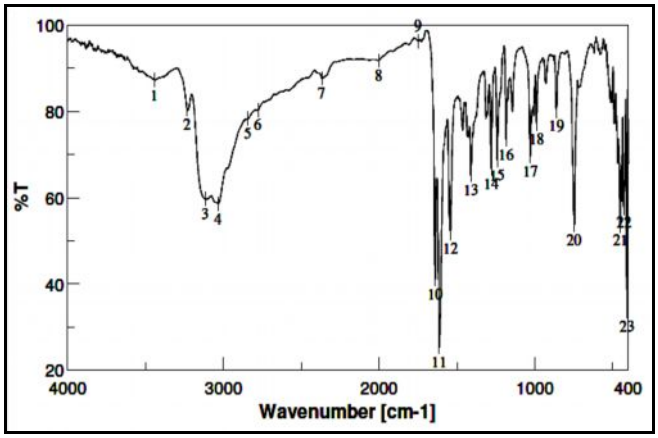

Figure. 2: FTIR Spectrum of PPCC

NMR spectral analysis

The ^{1}H NMR spectral features reveal the presence of different hydrogens of N-(2-pyridyl)piperazinium cation (Figure 3). The total of 8 protons corresponding to CH_2 protons of piperazine molecule observed in the range of 3.1- 3.9 ppm. The aromatic protons of pyridyl group occur in the region of 6.9-8.1 ppm including a single proton at 8.1 and 7.3 ppm which are assigned to H2 and H5 of the pyridine ring respectively. The other two aromatic protons exhibit peaks at 6.9 and 7.9 ppm. All the signals correlate very well with those of the cation, N-(2-pyridyl)piperazine. The singlet peak observed at 9.4 ppm is associated with the NH_2^+ proton which confirms the protonation of N in the organic molecule to form the cation in PPCC.

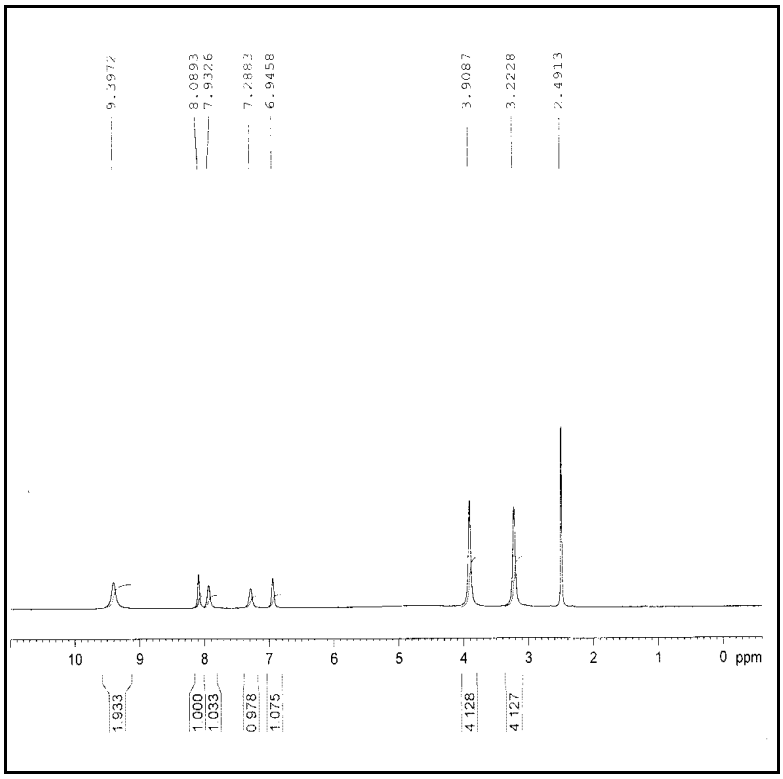

Figure. 3: ^{1}H NMR spectrum of PPCC

TGA/DTA analysis

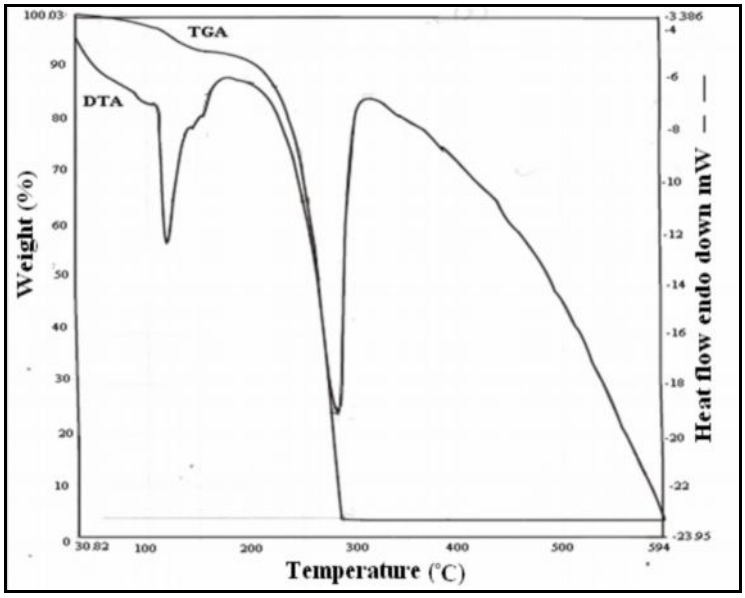

Figure. 4: TGA-DTA curves of PPCC

The TGA/DTA spectrum is presented in Figure 4, (Table 1) shows that it loses two molecules of hydrogen chloride between 54 and 241 ^{o}C. The percentage of hydrogen chloride calculated (18%) correlates with the experimental value (14%). The DTA curve reveal that there is a massive endothermic heat change from 241 °C to 300 °C with the peak at 282 °C and a mass loss of 83% (cal; 80%). The crystal compound is decomposes in three stages with inflection points at 118, 165 and 282 ^{o}C. As the crystal structure has been established, its molecular formula is $C_9H_{15}Cl_4CuN_3$. Calculations were made on the basis of mass loss using the above formula. The ΔH value for the process is 539.55 J/g. As the value is greater than that for HCl liberation, this decomposition consumes greater energy.

Table 1: Thermal behavior of PPCC

Temperature range °C	Inflexion Point °C	ΔH value J/g	Endo/ Exothermic	Liberation of Process
54-150	118	139.92	Endo	2HCl
150-241	165		Endo	Phase transition 1-(2-pyridylpiperazine)
241-300	282	539.55	Endo	$CuCl_2$
300-600	----		----	

Table 2: Crystal data and structure refinement for PPCC

Identification code	**Shelxl data** [CCDC 883154]
Empirical formula	$C_9 H_{15} Cl_4 Cu N_3$
Formula weight	370.58
Temperature	293(2) K
Wavelength of X-ray	0.71073 A
Crystal system, space group	Monoclinic, $P2_1/c$
Unit cell dimensions	a = 9.194(5) Å; alpha = 90.000(5) (°) b = 16.152(5) Å; beta = 99.254(5) (°) c = 9.471(5) Å; gamma = 90.000(5) (°)
Volume	1388.2(11) ($Å^3$)
Z, Calculated density	4, 1.773 (mg/m^3)
Absorption coefficient	2.324 mm^{-1}
F(000)	748
Crystal size	0.30 x 0.20 x 0.20 mm
Theta range for data collection	2.52 to 25.00 deg.
Limiting indices	-10<=h<=10, -19<=k<=19, -11<=l<=11
Reflections collected / unique	13086 / 2439 [R(int) = 0.0283]
Completeness to theta = 25.00	100.0 %
Absorption correction	Semi-empirical from equivalents
Refinement method	Full-matrix least-squares on F^2
Data / restraints / parameters	2439 / 3 / 167
Goodness-of-fit on F-2	1.054
Final R indices [I>2sigma(I)]	R1 = 0.0236, wR2 = 0.0584
R indices (all data)	R1 = 0.0265, wR2 = 0.0608
Extinction coefficient	0.0117(6)
Largest diff. peak and hole	0.736 and -0.755 $e.A^{-3}$

Table 3: Bond lengths (Å)

Bond	**Length**	**Bond**	**Length**
C(1)-N(1)	1.344(3)	C(7)-H(7A)	0.9700
C(1)-N(2)	1.348(3)	C(7)-H(7B)	0.9700

C(1)-C(2)	1.405(3)	C(8)-N(3)	1.490(3)
C(2)-C(3)	1.361(3)	C(8)-C(9)	1.504(4)
C(2)-H(2)	0.9300	C(8)-H(8A)	0.9700
C(3)-C(4)	1.381(4)	C(8)-H(8B)	0.9700
C(3)-H(3)	0.9300	C(9)-N(2)	1.460(3)
C(4)-C(5)	1.352(4)	C(9)-H(9A)	0.9700
C(4)-H(4)	0.9300	C(9)-H(9B)	0.9700
C(5)-N(1)	1.350(3)	N(1)-H(1A)	0.813(17)
C(5)-H(5)	0.9300	N(3)-H(3A)	0.871(17)
C(6)-N(2)	1.462(3)	N(3)-H(3B)	0.859(17)
C(6)-C(7)	1.504(3)	Cl(1)-Cu(1)	2.2823(9)
C(6)-H(6A)	0.9700	Cl(2)-Cu(1)	2.2787(9)
C(6)-H(6B)	0.9700	Cl(3)-Cu(1)	2.3083(13)
C(7)-N(3)	1.489(3)	Cl(4)-Cu(1)	2.2363(11)

Table 4: Bond angles (°)

Angle	Values (deg)	Angle	Values (deg)
N(1)-C(1)-N(2)	120.2(2)	C(9)-C(8)-H(8A)	109.7
N(1)-C(1)-C(2)	116.3(2)	N(3)-C(8)-H(8B)	109.7
N(2)-C(1)-C(2)	123.4(2)	C(9)-C(8)-H(8B)	109.7
C(3)-C(2)-C(1)	119.7(2)	H(8A)-C(8)-H(8B)	108.2
C(3)-C(2)-H(2)	120.1	N(2)-C(9)-C(8)	110.8(2)
C(1)-C(2)-H(2)	120.1	N(2)-C(6)-H(9A)	109.5
C(2)-C(3)-C(4)	121.9(2)	C(8)-C(9)-H(9A)	109.5
C(2)-C(3)-C(4)	119.1	N(2)-C(9)-H(9B)	109.5
C(4)-C(3)-H(3)	119.1	C(8)-C(9)-H(9B)	109.5
C(5)-C(4)-C(3)	117.7(2)	H(9A)-C(9)-H(9B)	108.1
C(5)-C(4)-H(4)	121.1	C(1)-N(1)-C(5)	124.2(2)
C(3)-C(4)-H(4)	121.1	C(1)-N(1)-H(1A)	122(2)
N(1)-C(5)-C(4)	120.2(2)	C(5)-N(1)-H(1A)	114(2)
N(1)-C(5)-H(5)	119.9	C(1)-N(2)-C(9)	122.63(19)
C(4)-C(5)-H(5)	119.9	C(1)-N(2)-C(6)	123.77(19)
N(2)-C(6)-C(7)	110.43(19)	C(9)-N(2)-C(6)	110.84(18)
N(2)-C(6)-H(6A)	109.6	C(7)-N(3)-C(8)	112.92(18)
C(7)-C(6)-H(6A)	109.6	C(7)-N(3)-H(3A)	111.8(19)
N(2)-C(6)-H(6B)	109.6	C(8)-N(3)-H(3A)	106.0(19)
C(7)-C(6)-H(6B)	109.6	C(7)-N(3)-H(3B)	110(2)
H(6A)-C(6)-H(6B)	108.1	C(8)-N(3)-H(3B)	111(2)
N(3)-C(7)-C(6)	109.13(19)	H(3A)-N(3)-H(3B)	105(3)
N(3)-C(7)-H(7A)	109.9	Cl(4)-Cu(1)-Cl(2)	163.49(3)
C(6)-C(7)-H(7A)	109.9	Cl(4)-Cu(1)-Cl(1)	93.75(4)
N(3)-C(7)-H(7B)	109.9	Cl(2)-Cu(1)-Cl(1)	92.13(4)
C(6)-C(7)-H(7B)	109.9	Cl(4)-Cu(1)-Cl(3)	92.98(4)
H(7A)-C(7)-H(7B)	108.3	Cl(2)-Cu(1)-Cl(3)	92.91(3)
N(3)-C(8)-C(9)	110.02	Cl(1)-Cu(1)-Cl(3)	138.11(3)
N(3)-C(8)-H(8A)	109.7	---	---

Crystal structure

The crystal data and the refinement parameters of PPCC are presented in Table 2. The selected bond lengths in Table 3 and bond angles in Table 4 are provided. The title compound PPCC crystallizes in monoclinic system with space group P21/c and refined to give final R value of 0.0236. The copper atom

exhibits a distorted trigonal bipyramidal geometry consisting of 2 equatorial Cl atoms (Cl1, Cl3) and two Cl atoms (Cl2, Cl4) at nearly axial positions. The Optimized structure of PPCC is presented in Figure 5. The asymmetric unit consists of a dimeric anion and a $[(N\text{-}(2\text{-}pypipzH_2))]^{2+}$ dication. The piperazine moiety of cationic part adopts chair conformation where the pyridyl and the piperazine are twisted in the N-C-N reference plane. The dimeric anions are well separated from a, b and c directions. The ORTEP diagram of PPCC is illustrated in Figure 6. The $Cu_2Cl_8^{4-}$ anion is discrete and exists as a bifolded centro-symmetric dimer.

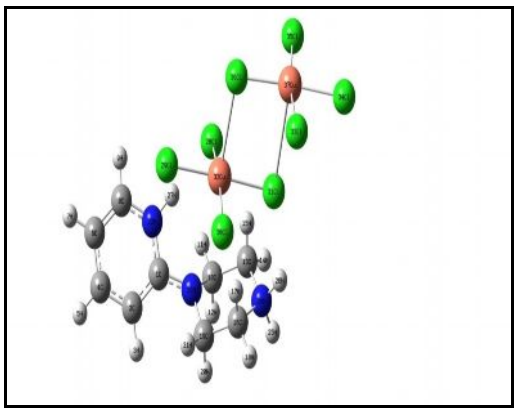

Figure. 5: Optimized geometry of PPCC

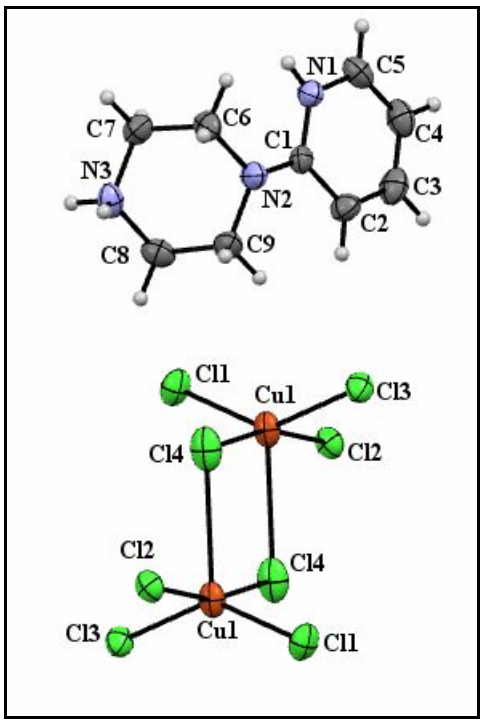

Figure. 6: ORTEP diagram with the atom labeling scheme

The structure of anionic dimer contains two four coordinated Cu(II) ions with highly distorted trigonal bipyramidal $CuCl_4^{2-}$ units sharing an edge formed by one axial and one equatorial corner about the Cu atom and two of which are involved in bridging. The geometry of the anion may be described as a distorted trigonal bipyramid having 2 equatorial Cl atoms (Cl1, Cl3) and two Cl atoms (Cl2, Cl4) at nearly axial positions. The Cu1-Cl4-Cu1-Cl2 moiety lies in one plane with the anionic dimer having an inversion centre. The bridging Cl4 atom is axial to one copper and equatorial to the other copper atom. There is no bonding between the two copper atoms. The distance of Cu-Cu is 3.935 Å being higher than the Cu-Cu distance of 3.722 Å as reported[11] and also greater than the values found in other dimers[27]. Moreover, the Cl4-Cl4 distance, 3.445 Å, is somewhat larger than the distances found for other compounds containing Cl-Cl chlorine bridges with the value falling within the range of 3.05-3.35 Å[28].

The Cu-Cl4 bonds of the two $CuCl_4^{2-}$ units are involved in bridging to form a $Cu_2Cl_8^{4-}$ anion with Cl2-Cu-Cl4 being nearly linear with an angle of 163.49 Å, which is closer to the normal linear angle 180 Å between

the tips of pyramids. The angle of 138.1˚ is observed for Cl1-Cu1-Cl3. The average bond angle of 112.46˚ for Cl-Cu-Cl in the triangular plane is closer to the value of trigonal angle 120 Å.

The intradimer bridging angles are Cl4-Cu1-Cl1 and 92.13˚ Cl2-Cu1-Cl1 are 90.75° and 92.15° respectively which are similar to those observed for other chlorocuprate(II)[11]. The higher trigonal angle, being greater than the value of the 90˚ reveals that the geometry at Cu is explained as being a distorted trigonal bipyramidal in the dimeric structure. The dihedral angle between the $CuCl_2$ planes is 89.04˚(2) Å, commensurate with distorted trigonal bipyramid geometry. The bond lengths of the bridging Cu-Cl bonds are 2.236 Å and 2.945 Å and the terminal Cu-Cl distances are 2.279 Å, 2.282 Å and 2.308 Å which are similar to the reported values[11]. The bridging Cu-Cl distance is 2.236 Å and is slightly (0.04 Å) less than the other three terminal ones of Cu-Cl2 (2.279 Å) Cu-Cl1 (2.282 Å) and Cu-Cl3 (2.308 Å) as a result of Jahn-Teller distortion[27].

The Cu-Cl bond distances of the dimer are similar to the reported values with distances of 2.285 and 2.239 Å with the average Cu-Cl distance of 2.514 in $Cu_2Cl_8^{4-}$ unit[11]. The Cl4-Cu1 distance differs appreciably more by 0.04 Å (2.2363Å) and less than the other three longer Cu-Cl distances of Cl1-Cu1 (2.2823 Å), Cl2-Cu1 (2.2787 Å) and Cl3-Cu1 (2.3083 Å). The values are relatively lower than the Ni-Cl distances found in $Ni_2Cl_8^{4-}$ moiety, 2.366 Å & 2.449 Å and still lower than the value of 2.703 Å, found in $Cu_2Cl_8^{4-}$ moiety where the average Cu-Cl bridged bond length is 2.514 Å [29,30].

The unequal distances result from molecular association through hydrogen bonding[30] which stabilizes the distorted geometry of $Cu_2Cl_8^{4-}$ anion in the dimer and makes the cationic ring much more puckered as noticed in other chlorocuprate(II)[11]. Table 5 illustrate the extensive hydrogen bonding network between the chlorine atoms of tetrachlorocuprate(II) and the cation moiety.

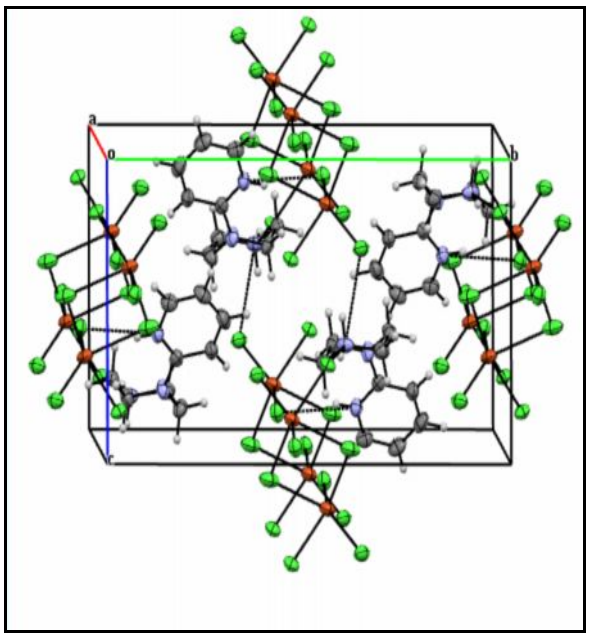

Figure. 7: Packing diagram of PPCC along with the hydrogen bonding. Hydrogen bonds are shown in dotted lines.

The molecular packing diagram for PPCC is depicted in Figure 7. The cationic species form discrete layers between dimeric anionic layers with an alternate arrangement between them. The stability of the compound depends on the extensive H-bonding networks between the cations and the anions. One N(3) atom of piperazine forms two single H-bonds to Cl of separate anions. Each anion has four cations around with an individual being bonded to different chlorine through the two $CuCl_4^{2-}$ units of the dimer. The two independent trans Cl-Cu-Cl angles are found to have values of 163.49(3) and 138.1(3) with an average of 150.795 Å.

Table 5: Hydrogen bonds (Å and °)

D-H...A	d(D-H)	d(H...A)	d(D...A)	∠(DHA)
N(3)-H(3A)...Cl(1)[a]	0.871(17)	2.43(2)	3.216(3)	150(2)
N(3)-H(3A)...Cl(2)[a]	0.871(17)	2.85(2)	3.504(2)	134(2)
N(3)-H(3B)...Cl(2)[b]	0.859(17)	2.416(19)	3.245(3)	162(3)
N(3)-H(3B)...Cl(4)[c]	0.859(17)	2.92(3)	3.400(3)	118(2)
N(1)-H(1A)...Cl(3)[d]	0.813(17)	2.389(19)	3.173(2)	162(3)

symmetry transformations used to generate equivalent atoms:
[a] x,-y+1/2,z+1/2 [b]-x+2,y-1/2,-z+3/2 [c]x,-y+1/2,z-1/2 [d]-x+1,y-1/2,-z+3/2

The hydrogen atoms attached to N1 and N3 are involved in hydrogen bonding with Cl1, Cl2, Cl3 and Cl4 (Table 5). It is interesting to note that the dimeric anion, $Cu_2Cl_8^{4-}$ has an inversion center coinciding with the center of the dimer. This may be due to effective H-bonds which flatten the structure. The increase in the abilities of organic cations to form H-bonds with the anion leads to the increase in distortion of its tetrahedral geometry and thus the dimerisation of $CuCl_4^{2-}$ anion results. The anionic is regarded as a distorted trigonal bipyramidal geometry assumed for attaining the hydrogen-bonding capabilities with the medium sized organic cations. The $Cu_2Cl_8^{4-}$ anion is isolated from cationic species and exists as a centro-symmetric dimer stabilized by H-bonds. The strong hydrogen bonding, exhibited by N3-H3A….Cl2, has the donor-acceptor distance of 3.504(2) Å (Table 5)

Antibacterial activity

The zone of bacterial growth inhibition by PPCC against *Staphylococcus aureus, Pseudomonas aeruginosa* as well as *Eschrichia coli* shows a stronger effect against tetracycline used as standard. The lowest concentration (highest dilution) required to arrest the growth of bacteria was regarded as minimum inhibitory concentration (MIC). The diameter of the zone of inhibition and minimum inhibitory concentration values were given in Table 6.

Table 6: The diameter of the zone of inhibition and minimum inhibitory concentration shown by PPCC against *Escherichia coli*, *Staphylococcus aureus* and *Pseudomonas aeruginosa*

Organism	Inhibition zone (mm)	Control (tetracycline)
Escherichia coli	2.0±1.66	1.5±5.63
Staphylococcus aureus *Pseudomonas aeruginosa*	*2.0±2.16* *2.0±1.6*	1.5±4.37 1.5±5

Antifungal activity

Antifungal activity was exhibited by PPCC against fungal plant pathogens, *Colletotrichum* and *Fusarium* species, as revealed by the zone of fungal growth inhibition in two different concentrations (100 and 50 µL). The two species were more sensitive to the 100 µL concentration than 50 µL level employed. The test results presented in Table 7 showed that the complex causes considerable activity against *Colletotrichum* and *Fusarium* species. The reduction of inhibition zone was noticed with lowering of concentration of PPCC placed on the fungal culture. The strong antifungal activity of PPCC might be due to the presence of hetero atom in heterocyclic amine moiety of the complex.

Table 7: Antifungal activity of PPCC against *Colletotrichum* and *Fusarium* species

Compound	Zone of inhibition (mm) *Colletotrichum/Fusarium* Concentration(µL)		
	50 µL/ mL	100 µL/ mL	Control
PPCC	38/22	28/23	60/50

HOMO-LUMO analysis

The orbital energy level analysis for PPCC reveals values of +0.003 and -0.003 eV for E_{HOMO} (highest occupied molecular orbital) and E_{LUMO} (lowest unoccupied molecular orbital) respectively. The LUMO is spread largely on two chlorine atoms. HOMO appears to disperse over the bridging chlorine atoms as well as the piperazine unit of the cationic organic molecule. The magnitude of the HOMO-LUMO energy separation is a measure of the reactivity pattern of the molecule and an indicator of the kinetic stability[31]. Thus, the compound has a small HOMO-LUMO gap of 0.002eV implying lower kinetic stability and a higher chemical reactivity. The values of charge density for PPCC lie in the range of -6.334 e^{-2} to 6.334 e^{-2} and are equally distributed over the entire molecule. The orbital contours of HOMO and that of LUMO of the molecule are shown in Figures 8. The charge density (Figure 9) is distributed such that maximum densities are found in the regions where chlorine atoms and nitrogen atoms are present in agreement with their greater electronegativities.

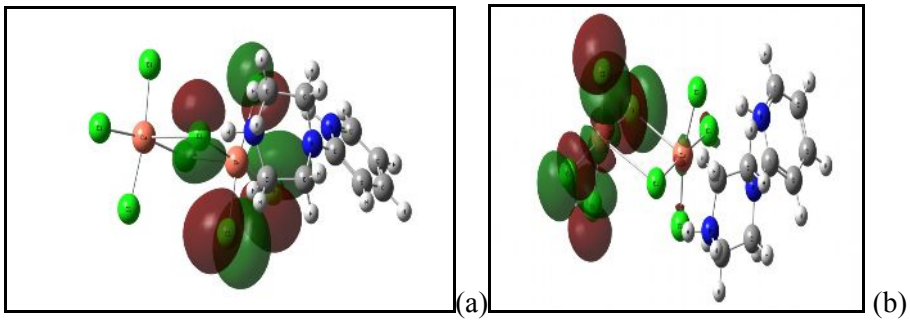
(a) (b)

Figure. 8: Orbital Contours of HOMO (a) and LUMO (b) for PPCC

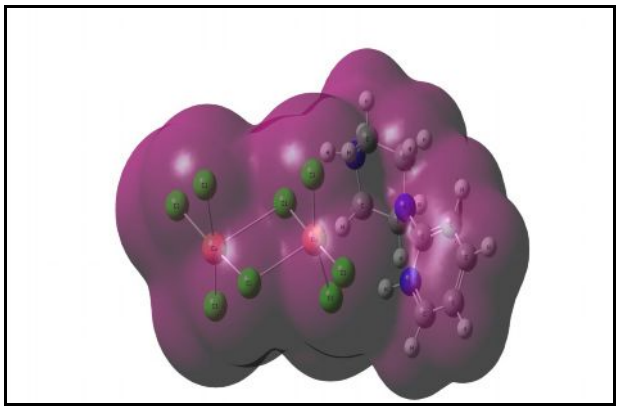

Figure. 9: Total charge density for PPCC

A close scrutiny reveals that the experimental values for the lengths of C-Cl linkages in the crystal are 1.736 Å and 1.738 Å in comparison to the closely occurring calculated values of 1.7550 Å and 1.7581 Å showing deviations of +0.019 Å and +0.0201 Å respectively. A similar trend is observed for C-N and C-C bonds too with smaller deviations. The two O-H experimental bond distances are 0.9780 Å and 0.9608 Å may be attributed to the H-bonding between N-H and the more electronegative chlorine atom. The other bonds, such as C-C and N-C, experience very small deviations in the range of 1.373 Å to 0.978 Å.

However, larger deviations are observed for bond angles. The Cl2-Cu-Cl4 angle of 163.49˚ is closer to 180˚. The intradimer bridging angles of 93.75˚ (Cl4-Cu1-Cl1) and 92.13˚ (Cl2-Cu1-Cl1) are greater than the actual value of the 90˚. This suggests that the linkages are involved either directly or indirectly in hydrogen bonding in the condensed solid phase. Such deviations from the predicted angles for the gaseous complex can be taken as a measure of the intermolecular interactions. In the present system, the deviation can be attributed to the configurational changes required to make hydrogen bonding more effective in the crystal.

Conclusion

The salt N-(2-pyridyl)piperazinium tetrachlorocuprate(II) has been synthesized and characterized. The FT-IR study substantiates the nature of the cations. X-ray, ^{1}HNMR, UV-Visible spectral analyses reveal the geometries of the tetrachlorocuprate(II) anion as well as the cation. Thermogravimetric analysis of the

tetrachlorocuprate(II) revealed the liberation of HCl, N-(2-pyridyl)piperazine and $CuCl_2$ molecules which is consistent with the molecular formula. The single crystal XRD results reveal that it is monoclinic with space group of P21/c. The tetrachlorocuprate(II) anion of PPCC prefers a trigonalbipyramidal geometry and exists as a dimeric $Cu_2Cl_8^{4-}$ anion. The anion appears to be stabilized by very strong and extensive hydrogen bonding with the N-(2-pyridyl)piperazinium cation. The optimized data were employed to arrive at charge density distribution and HOMO-LUMO calculations. Inhibitory activities were observed against two bacterial species of *S.aureus*. *P. aeruginosa* and *E.coli* and two fungal pathogens viz., *Colletotrichum* and *Fusarium* species. The chlorocuprate(II) showed better activity than the control which may probably due to the hetero atom present in the ligand.

Supplementary Data

The entire X-ray crystal data have been deposited at the Cambridge Crystallographic Data Centre. CCDC 883154 contains the supplementary crystallographic data for N-(2-pyridyl)piperazine ligand and N-(2 pyridyl)piperazinium tetrachlorocuprate(II) complex; 12 Union Road, Cambridge CB2 1EZ, UK; fax: +44 1223 336 033.

Acknowledgement

The authors thank the Management, Thiagarajar College, Madurai-9, India and Syngene International Ltd., a Biocon company, Bangalore-99, India for permitting N. Dhanam to carry out the research work, Analytical and Instrumentation Facilities. We thank National Centre for Catalysis Research, Indian Institute of Technology, Chennai for providing computational facilities and solving the crystal structure and University of Delhi for TGA/DTA instrumental facility.

References

1. Atherden L.H., 'Bentley and Driver's Text Book of Pharmaceutical Chemistry'. Oxford Medicinal Publication 8th Edition (2004); 372 (20): 4.
2. Patrik G.L., An Introduction to Medicinal Chemistry, 2nd edition, Oxford University Press. (2001) 1.
3. Kharitonov D.N. and Golubeva E.N., Kinetics and Catalysis, (2005); 46: 52.
4. Natarajan M. and Prakash B., Phys. Status solidi(a) (1971); 4: K167-K172.
5. Yu Jie-Hui, Xu Ji-Qing, Song Yu-Jiang, Bie Hai-Ying, Lu Jing and Wang Tie-Gang, Chinese J. of Chem, (2005); 23: 1030.
6. Bhattacharya R., Ray M.S, Dey R., Righi L., Bocelli G., and Ghosh A., Polyhedron (2002); 21: 2561.
7. Akira O., Yoichi N., Tetsuya K. and Kazuhisa K., Condensed Matter (2005); 1-2: arXiv, cond-mat/ 0511179 (English).
8. Antolini L., Benedetti A., Febretti A.C. and Giusti A., Inorg. Chem, (1988); 27: 2192.
9. Byrappa K., Kandhaswamy M.A. and Srinivasan V., Cryst. Res. Tech, (1999); 34: 143.
10. Helmholz L. and Kruh R.F., J. Am. Chem. Soc, (1952); 74: 1176.
11. Anderson D.N. and Willet R.D., Inorg. Chim. Acta (1974); 8: 167.
12. Hodgson D.J., Hale P.K. and Hatfield W.E., Inorg. Chem, (1971); 10: 1061
13. Stratemeier H. and Hitchman M.A., Inorg. Chem, (1994); 33: 2320.
14. Haddad S. and Willett R.D., Inorg. Chem, (2001); 40: 2457.
15. Antolini L., Menabue L., Pellacani G. and Saladini M., Inorg. Chim. Acta (1982); 58: 193.
16. Jotham R.W. and Kettle S.F.A., Inorg. Chim. Acta (1971); 5: 183.
17. Lohr L.L., Jr and Lipscomb W.N., Inorg. Chem, (1974); 38: 255.
18. Suarez R.C., Santamarıa S.M. and Avendano C., Acta Cryst, (2000); C56: 385.
19. Sheldrick G.M., SHELXS97 and SHELXL97, University of Gottingen, Germany (1997).
20. Peng C., Ayala P.Y., Schlegal H.B. and Frisch M.J., J. Comp. Chem, (1996); 17: 49.
21. Frisch M.J., Trucks G.W., Schlegel H.B., Scuseria G.E. and Robb J.A., Gaussian 98, Revision A.9, Gaussian Inc., Pittsburgh, PA, 2001.
22. Willett J.C., Idone V.P., Orville R.E., Leteinturier C., Berard A.E., Barret L. and Krider E.P., J. Geophysical Research (1988); 93: 3867.
23. Mark E., Vol'pin E., Novodarova G.N., Krainova N.Yu., Lapikova V.P., and Andrey A., Journal of Inorganic Biochemistry (2000); 81: 285.
24. Geary W.J., Co-ord chemistry (1971) 81.
25. K. Robert, Bogges and David A., J of chemical education (1975); 649.

26. Wasson J. R, Hall J.W, Richardson H.W. and Hatfield W.E., Inorg Chem, (1977); 16: 458.
27. Koval I.A., Huisman M., Stassen A.F., Gamez P., Lutz M., Spekn A.L. and Reedijk J., Eur. J. Inorg. Chem, (2004); 591.
28. Smith D.W., Coord. Chem. Rev, (1976); 21: 93.
29. Barclay G.A. and Kennard C.H.L., J. Chem. Soc, (1961). 5244
30. Ross F.K. and Stucky G.D., J. Am. Chem. Soc, (1970); 92: 4538.
31. Chattopadhyay B., Basu S., Chakraborty P., Choudhury S. K., Mukherjee A.K, and Mukherjee M., J. Mol. Struct, (2009); 932: 90.

*****